ELSEVIER

Catalysis Today 68 (2001) 255–262

CATALYSIS TODAY

www.elsevier.com/locate/cattod

Adsorption and catalytic combustion of aromatics on platinum-supported MCM-41 materials

Q.-H. Xia, K. Hidajat, S. Kawi*

Department of Chemical and Environmental Engineering, National University of Singapore, 10 Kent Ridge Crescent, Singapore 119260, Singapore

Abstract

Among a series of Pt-supported catalysts prepared by impregnation, the most hydrophobic Pt-supported on MCM-41 (synthesized in the presence of fluoride anions) with large surface area and pore size is found to be the most active catalyst for the combustion of toluene in air, and its activity is maintained even in the presence of water. However, Pt/ZSM-5 with micropores, the smallest pore volume and the least hydrophobicity has the worst catalytic activity. The high oxidation activity of the catalyst depends mainly on its high hydrophobicity (characterized by selective adsorption for H_2O and toluene and by FTIR spectra of surface hydroxyl groups) and partly on its large pore size and high Pt loading. The order of the oxidation activity of a series of aromatics with different molecular weight and different boiling point on Pt-supported MCM-41 catalyst is found to be as follows: toluene > benzene > cumene > ethyl benzene > mesitylene.

Keywords: Catalytic combustion of aromatics; Pt/MCM-41; Pt-supported catalysts; Impregnation; Synthesis of MCM-41; Oxidation

1. Introduction

The volatile organic compounds (VOCs) have long been a major source of air pollution, and in many cases, legislation has already been introduced to reduce their emission [1–7]. These VOC contaminated gas streams are vented from a variety of industrial and commercial processes. The desired reaction is the complete combustion of VOC to CO_2 and H_2O [2].

The applications of hydrophobic (organophilic) catalyst are still in the development stage [8–12]. One of its applications is the deep oxidation of VOC. In order to minimize the energy consumption and to cut down the cost, it is required that the reaction temperature is as low as possible, and the catalyst can be cycled and regenerated many times. However, at low temperature, the water vapor generated from VOC oxidation can be easily condensed in the micro/meso-pores of metal oxide support, drastically reducing the catalyst activity. It is, therefore, of great interest to synthesize the hydrophobic catalyst having high VOC adsorption capacity and oxidation activity.

In conventional preparation of Pt-supported catalysts used in catalytic oxidations of hydrocarbons, porous inorganic materials containing a complex pore structure SiO_2, γ-Al_2O_3, α-Al_2O_3, TiO_2, MnO_2 and monolith [2,3,13–15], as well as microporous silicalite (pentasil zeolite) [10] are frequently used as carriers, which are generally acknowledged as low temperature catalysts. Volter et al. [5] showed that the oxidation on Pt occurred faster in air than in pure oxygen due to the formation of a relatively inactive "oxidic" [Pt^{IV}] species in highly oxidizing environments.

MCM-41 materials discovered by Mobil researchers [16] have great potentials as hydrophobic adsorbents [17] and catalysts for the catalytic destruction of VOC due to their high surface area (>1000 m^2/g),

* Corresponding author. Tel.: +65-874-6312; fax: +65-779-1936.
E-mail address: chekawis@nus.edu.sg (S. Kawi).

0920-5861/01/$ – see front matter
PII: S0920-5861(01)00285-1

large pore size (15–100 Å) and large pore volume (>0.9 cm^3/g). It is also known that fluorided silica surface is much more hydrophobic than a silanol silica surface [18]. Recently, Xia et al. [19] reported the formation of MCM-41 in fluoride medium that leads to the improvement of its hydrophobicity and hydrothermal stability. The aim of this work is to synthesize Pt-catalysts supported on various supports having different properties (such as hydrophobicity, pore size and pore volume) and to compare their catalytic activities for the combustion of aromatics.

2. Experimental

2.1. Synthesis of supports

The raw materials used were as follows: aerosil silica (99.9 wt.%, Merck), Ludox (40 wt.%, Aldrich), NaOH (98 wt.%, Merck), cetyltrimethyl ammonium bromide (CTMABr, pure, Merck), CTMAOH (self-made), $NaAlO_2$ (99 wt.%, Hanawa, Japan), tetraethyl ammonium hydroxide (TEAOH, 20 wt.%, Merck), hydrofluoric acid (40 wt.%, Merck), toluene, benzene, cumene, ethyl benzene and mesitylene (all are HPLC grades, Merck).

The synthesis of siliceous MCM-41 (M1) in the presence of fluoride anions was carried out according to the procedures reported elsewhere [19]. Siliceous (M2) and Al-containing MCM-41 (M3) materials were synthesized without fluoride anions according to the slightly changed recipes reported in the literature [20]. The Si/Al molar ratio in Al-containing MCM-41 was about 15. Na-form ZSM-5 (Si/Al = 25) was a commercial product.

2.2. Preparation of Pt-supported catalysts

Pt-supported catalysts with a Pt loading of 2 wt.% (Pt-2/M1) or 0.65 wt.% (Pt-0.65/M1) were prepared by impregnation method as follows: 2 g of powder supports pre-dried at 300°C overnight were added into a certain amount of 0.1 M $Pt(NH_3)_4(NO_3)_2$ solution and the mixture was vigorously stirred at room temperature for 24 h. Then the suspension was dried at 60°C overnight, followed by calcination at 550°C for 10 h in flowing air. Finally, the solid powder was pressed into wafer under the pressure of 1 tonne cm^{-2}, crushed and sieved into 20–40 mesh pellets. The same method was used to prepare Pt/M2, Pt/M3 and Pt/ZSM-5 with the same Pt loading of 2 wt.%.

2.3. Characterization of prepared catalysts

The XRD patterns of the prepared catalysts were measured using a Shimadzu XRD-6000 Spectrometer (Cu target/40 kV/30 mA). The elemental composition of the catalysts was measured by atomic absorption spectrophotometer (Shimadzu AA-670). The N_2 isotherms were measured by AUTOSORB-1 (Quantachrome) at 77.35 K. Prior to N_2 adsorption analysis, the samples were degassed at 573 K for 5 h. The pore diameter was calculated based on desorption branch by BJH method for the MCM-41 samples and by HK method for the ZSM-5 sample, respectively. The dynamic adsorption tests of water or toluene were performed on a Shimadzu DTG-50 thermogravimetric analyzer. The solid powder was placed onto an aluminium pan and heated in a flow of N_2 or He (62 ml/min) to 623 K at 15 K/min and maintained at 623 K for 200 min to desorb water completely. Then the system was cooled down to room temperature in order to adsorb a certain concentration of adsorbate from a flowing gas until equilibrium had been reached. The adsorption capacity (wt.%) was calculated as (weight of the adsorbed adsorbate/weight of the adsorbent) × 100. FTIR spectra of hydroxyl groups were recorded using a Shimadzu FTIR-8700 spectrophotometer connected to a PFEIFFER vacuum system. Before scanning, the samples were pressed into thin wafers (10 mg cm^{-2}) under the pressure of 4 tonne cm^{-2} and evacuated under 1.0×10^{-6} mbar in an in situ IR cell at 200°C for 5 h. The dispersion of Pt metal species on the support was determined by equilibrium hydrogen chemisorption at room temperature using AUTOSORB-1 (Quantachrome). Prior to H_2 chemisorption analysis, the samples were evacuated at 200°C for 1 h, then exposed to static H_2 at 300°C for 2 h and finally placed under dynamic vacuum at 300°C for 3 h [15].

2.4. Catalytic combustion

Prior to testing of the catalysts, 0.4 ml of Pt-supported catalyst (i.e. 0.10 g for Pt/MCM catalyst and 0.20 g for Pt/ZSM-5 catalyst) was loaded into a glass reactor

and reduced in a flow of pure hydrogen at 400°C for 10 h. The organic reactants were carried into the reactor by flowing a stream of pure air through a bubbler to generate a constant organic concentration ranging from 4340 to 45,000 ppm. The reactions were carried out at temperatures ranging from 100 to 400°C under atmospheric pressure with a volume hourly space velocity (VHSV) of 15,000 h^{-1}. Before the conversion of each reaction was measured, the catalytic bed was stabilized under the feed stream at the required reaction temperature for 2 h. The products were analyzed in situ by Shimadzu 17A gas chromatograph equipped with an FID and a Porapak-Q capillary column. Major products in most experimental conditions were CO_2 and H_2O, with only a trace amount of other hydrocarbons, such as CH_4 and dimethyl benzene, being detected under some other conditions. The ignition curves of the catalysts were constructed based on the disappearance of the organic compounds.

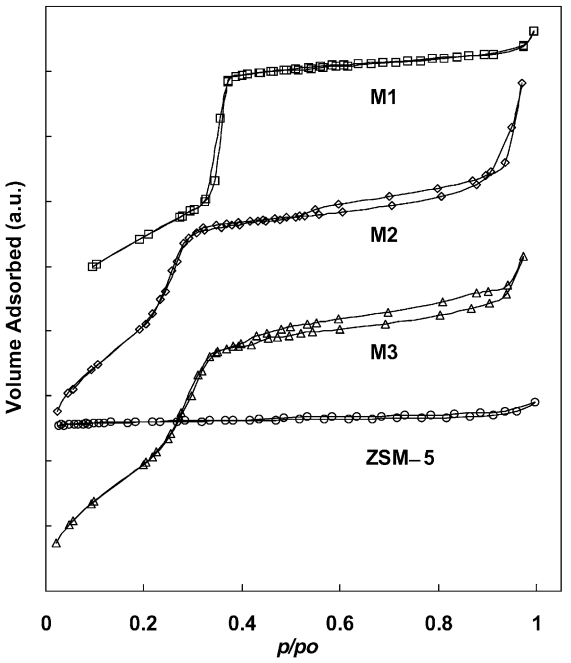

Fig. 1. Isotherms of N_2 adsorption/desorption of supports.

3. Results

3.1. Structure of supports

Fig. 1 displays the N_2 adsorption/desorption isotherms of MCM-41 and ZSM-5 support materials. A typical type IV isotherm of MCM-41 (having a sharp inflection at the relative pressure (P/P_o) between 0.25 and 0.40) is observed for samples M1, M2 and M3. ZSM-5 sample displays a Type I isotherm, which is a typical characteristic of microporous solids. The XRD patterns confirm that all synthesized materials, except ZSM-5, have typical MCM-41 mesoporous structure. However, the diffraction peaks corresponding to Miller indices (1 0 0), (1 1 0), (2 0 0) and (2 1 0) are sharper and more intense for samples synthesized in fluoride medium, indicating that these materials have more highly ordered pore structures [21].

Table 1 shows the material properties measured by BET and XRD. M1, M2 and M3 materials have large surface area, big pore size and pore volume. However, there are some differences in the 2θ value of the (1 0 0) diffraction peak of these MCM-41-type materials, indicating that they have different pore sizes. In addition, XRD patterns (measured with 2θ values from 1.5

Table 1
XRD measurements and BET analyses of supports

Support	BET (m^2/g)	Pore volume[a] (cm^3/g)	Pore diameter (Å)	Structure[b]	2θ (1 0 0)[b] (°)
M1	1077	0.95	29.7	MCM-41	2.15
M2	1279	1.15	26.0	MCM-41	2.56
M3	1287	0.96	26.9	MCM-41	2.48
ZSM-5	363	0.15	5.4[c]	ZSM-5	

[a] At $P/P_o = 0.90$.
[b] Determined by XRD.
[c] Estimated by HK method for desorption branch. The synthesis recipes of mother materials (molar ratio): sample M1, SiO_2:NaOH:CTMABr:H_2O:HF = 1:0.54:0.50:100:0.34; M2, SiO_2:CTMAOH:H_2O = 1:0.97:65; M3, SiO_2:Al_2O_3:TEAOH:CTMAOH:H_2O = 1:0.0345:0.20:0.23:50.

Table 2
Adsorption data of supports and Pt content of catalysts[a]

Sample	Support	H_2O[b] adsorption	Toluene[c] adsorption	α[d]	Pt content (wt.%)	Pt dispersion (%)
Pt-2/M1	M1	3.0	20.1	6.70	2.05	77
Pt-0.65/M1	M1	3.0	20.1	6.70	0.65	84
Pt/M2	M2	15.1	20.5	1.36	2.07	75
Pt/M3	M3	19.6	18.0	0.92	2.10	79
Pt/ZSM-5	ZSM-5	10.3	6.5	0.63	1.99	39

[a] Pt-2/M1 and Pt-0.65/M1 used the same support M1.
[b] H_2O concentration (wt.%), 12,300 ppm.
[c] Toluene concentration (wt.%), 4200 ppm.
[d] Hydrophobic index (α): adsorption capacity (wt.%) of toluene/adsorption capacity (wt.%) of water.

to 60°) show that most of the Pt-supported samples, except Pt/ZSM-5, do not form any PtO_2 crystalline phase. In addition, Table 2 shows that the dispersion of Pt-supported on MCM-41 materials is very high (up to 75–84%), and those supported on ZSM-5 is relatively low (only 39%). The results show that Pt-species supported on MCM-41 materials are highly dispersed.

3.2. Adsorption of toluene and water on supports

Table 2 shows the respective adsorption capacities of supports M1, M2, M3, and ZSM-5 for water and toluene. All MCM-41-type samples can adsorb much more toluene than ZSM-5, which can be attributed to their larger surface area, bigger pore volume and pore size. Supports M2, M3 and ZSM-5 adsorbed more water than M1. This is not surprising as it is known that the surface framework containing a large quantity of Al is more hydrophilic than purely-siliceous surface framework [22], and a fluorided siliceous surface is more hydrophobic than the non-fluorided ones [18]. A hydrophobic index (α) is used in this study to quantify the hydrophobicity of the materials. The α-values for these materials are found to be in the following order: M1 > M2 > M3 > ZSM-5. The result shows that the hydrophobicity of the materials can be tuned by synthesis parameters, such as by the gel composition (with or without fluoride ions or aluminum ions).

To demonstrate further the effect of fluorination on the improvement of surface hydrophobicity, Fig. 2 shows the FTIR spectra characterizing the in situ vibrations of surface hydroxyl groups of various supports under high vacuum. The broad absorption band between 3000 and 3800 cm^{-1} corresponds to the fundamental stretching vibrations of different hydroxyl groups [18]. It is composed of a superposition of Si–OH stretching vibrations, such as isolated vicinal Si–OH stretching at about 3740 cm^{-1} and hydrogen-bonded Si–OH stretching at 3100–3680 cm^{-1}. The sharp vibration band at 3740 cm^{-1} can, therefore, be assigned to free hydroxyl stretching [23] and the broad band between 3100 and 3680 cm^{-1} to the hydrogen-bonded hydroxyl stretching. The result shows that the surface hydroxyl groups on M1 are mainly composed of isolated hydroxyl groups and most of those on the surface of M2 and M3 are

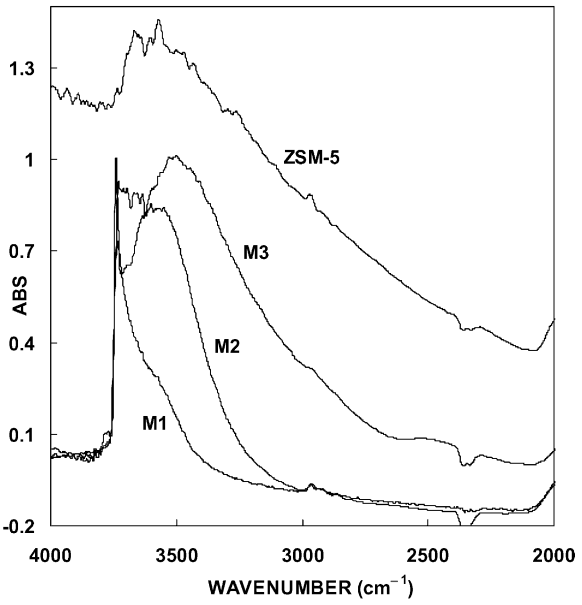

Fig. 2. FTIR spectra of –OH vibrations of different supports.

hydrogen-bonded hydroxyl groups. The density of surface hydroxyl groups is found to be in this order: M3 > M2 > M1 > ZSM-5. This order is in agreement with the uptake amount of water on these materials and the order of hydrophobicity index, reflecting the crucial effect of the density of surface hydroxyl groups on the adsorption of water.

Although ZSM-5 has much lower density of surface hydroxyl groups than M2 and M3, however, its α is also low. This may be explained by the limited diffusion of organic adsorbate and capillary condensation of water molecules in the pentasil micropores of ZSM-5, resulting in its high hydrophilicity.

3.3. Catalytic combustion of aromatics

Fig. 3 shows the activity of Pt-2/M1 catalyst for the oxidation of aromatic compounds at the concentration of 4340 ppm. For the five aromatic compounds used in this study, their molecular weights are in this order: mesitylene = cumene (120.2) > ethylbenzene (106.2) > toluene (92.1) > benzene (78.1), and their boiling points are in this order: mesitylene (165°C) > cumene (153°C) > ethylbenzene (136°C) > toluene (111°C) > benzene (80°C). However, the order for the oxidation reactivity of the above five compounds on the catalyst (i.e. toluene > benzene > cumene > ethylbenzene > mesitylene) does not follow the order based on their boiling points or molecular weights [11,24,25]. Toluene appears to be the most reactive, with 100% conversion achievable at about 150°C, at which temperature the other four compounds could only achieve a conversion less than 17%. For these compounds, a 100% conversion can only be achieved at higher temperatures: 220°C for benzene, 250°C for cumene, 300°C for ethylbenzene, and 350°C for mesitylene. Since the methyl group in the toluene aromatic ring is the most readily activated to form stable free radical or carbonium ion, the oxidation of toluene may quickly occur at low temperature. The fact that cumene is more easily oxidized than ethylbenzene may be explained by the same reasoning.

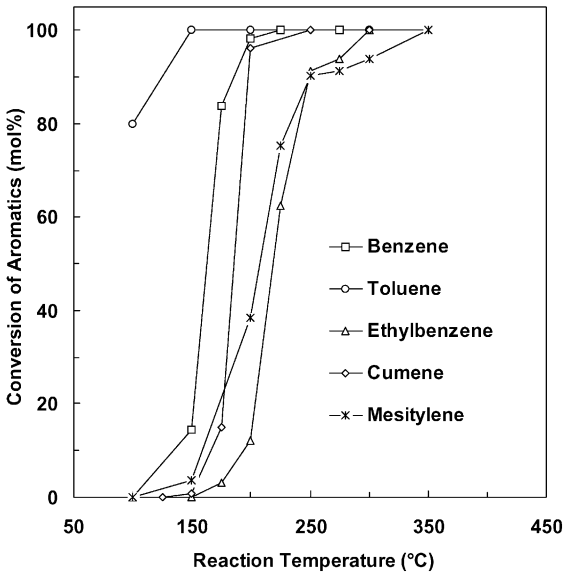

Fig. 3. Combustion of aromatics in air on Pt-2/M1. VHSV, 15,000 h^{-1}; concentration, 4340 ppm.

Wu et al. [11] obtained a high combustion activity for toluene on hydrophobic Pt-supported porous styrene divinylbenzene copolymer (SDB) catalyst under low toluene concentration (90 ppm) and low temperature (around 150°C). However, the total combustion temperature had to be increased to higher temperature (190°C) when the catalyst support was changed to activated carbon. They explained this result due to the difference in the hydrophobicity of the supports. Their results are in agreement with our present findings.

Based on Mars-Van-Krevelen mechanism for the oxidation of hydrocarbons [9], the reduced sites over supported Pt metal catalyst are generated by the oxidation of hydrocarbon. When a catalyst becomes hydrophobic, hydrocarbon can be more readily adsorbed on the catalyst surface for reaction. As a result of the reaction, there will be more active reduced sites generated on the catalyst surface. This effect is expected to be more profound for the deep oxidation of hydrocarbons, producing a lot more water which is an inhibitor for hydrocarbon oxidation. Therefore, Pt-2/M1 catalyst, which has the highest hydrophobic property, has shown the highest activity for the oxidation of toluene with or without the presence of water in the gas stream.

3.4. Catalytic combustion of toluene

3.4.1. Effect of Pt content

Fig. 4 shows a large difference in toluene oxidation activity between Pt-2/M1 and Pt-0.65/M1

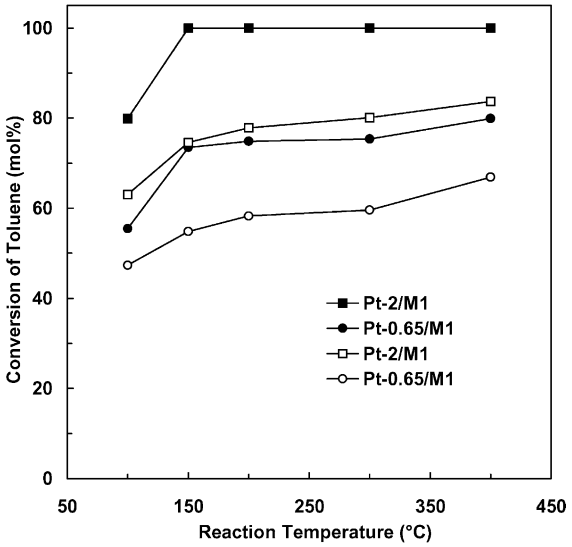

Fig. 4. Effect of Pt content on combustion of toluene in air. VHSV, 15,000 h^{-1} (toluene); solid symbol, 4340 ppm; open symbol, 45,000 ppm.

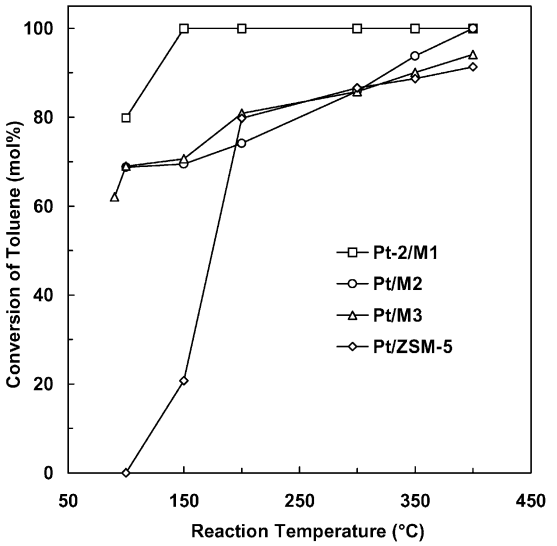

Fig. 5. Effect of temperature on combustion of toluene on different Pt-supported catalysts. VHSV, 15,000 h^{-1}; toluene, 4340 ppm.

having different Pt loading but almost similar Pt dispersion. Pt-2/M1 always has higher combustion activity than Pt-0.65/M1 regardless of the concentration of toluene and the reaction temperature. Since Pt-2/M1 contains three times more Pt than Pt-0.65/M1, the result shows that the high Pt loading can produce more catalytic sites which are active for the catalytic oxidation of toluene in air. This is in agreement with the results observed on conventional supported noble metals catalysts [2,4–7].

3.4.2. *Effect of temperature*

Fig. 5 shows a comparison of the combustion activity of toluene (under a concentration of 4340 ppm and VHSV of 15,000 h^{-1}) on all catalysts having 2 wt.% of Pt loading. Among the catalysts tested, Pt/ZSM-5 has the worst activity at low temperatures, even though, on the same volume basis, the Pt amount of the Pt/ZSM-5 catalyst is as twice as that of Pt/MCM-41 catalysts. At temperatures as low as 100°C, the conversion of toluene is almost close to 0, but when the reaction temperature is increased to ≥200°C, the oxidation activity is markedly improved. This result may be explained by the fact that due to capillary condensation, water (with a boiling point of 100°C) and toluene (with a boiling point of 111°C) can easily block the micropores (5.4 Å) of Pt/ZSM-5, preventing the occurrence of oxidation at low temperature. Furthermore, the micropores of ZSM-5 produces a low Pt dispersion (only 39%) on Pt/ZSM-5, leading to its low catalytic activity. For a comparison, the oxidation activity of Pt/MCM-41 catalysts has already reached more than 60% conversion at 100°C; this is possibly due to their high Pt dispersion (close to 80%) and the minimal diffusion resistance of reactant and product molecules into and out of the large pore of MCM-41-type catalysts. For all Pt/MCM-41 catalysts, the order of activity follows the hydrophobicity of the catalysts as follows: Pt-2/M1 > Pt/M2 ≈ Pt/M3. This result shows that hydrophobicity plays an important role in the catalyst activity for oxidation as the water produced during the reaction can be removed easily from the catalyst sites. However, when the temperature is over 300°C, the oxidation activity of Pt/M2 is significantly enhanced as compared to Pt/M3, indicating that the effect of hydrophobicity can be further enhanced at higher temperatures.

3.4.3. *Effect of additional H_2O in the gas stream*

Fig. 6 shows the effect of additional water in the gas stream on the catalyst activity (under 4340 ppm of toluene and 21,000 ppm of H_2O). The presence of

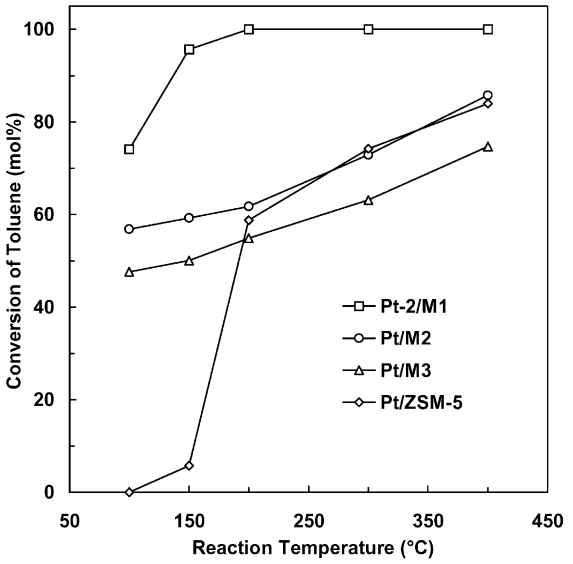

Fig. 6. Effect of H_2O on combustion of toluene over Pt-supported catalysts. VHSV, 15,000 h^{-1}; toluene, 4340 ppm; H_2O, 21,000 ppm.

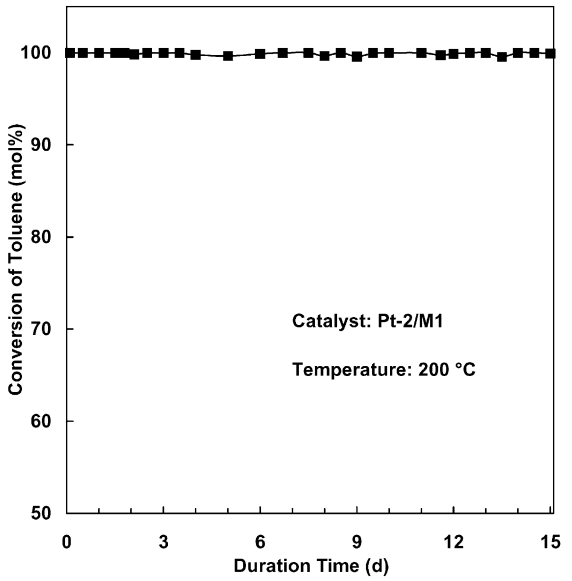

Fig. 7. Effect of H_2O on duration time of the catalyst Pt-2/M1 in combustion of toluene. VHSV, 15,000 h^{-1}; toluene, 4340 ppm; H_2O, 21,000 ppm.

the additional H_2O almost has no effect on the oxidation activity of Pt-2/M1 but significantly reduces the oxidation activity of Pt/M2, Pt/M3 and Pt/ZSM-5. At temperatures below 250°C, the oxidation activity of catalysts is found to be in this order: Pt-2/M1 > Pt/M2 > Pt/M3 > Pt/ZSM-5. However, once the temperature is increased to above 250°C, the oxidation activity of catalysts is found to be in this order: Pt-2/M1 > Pt/M2 ≈ Pt/ZSM-5 > Pt/M3. Fig. 7 shows the catalyst activity for Pt-2/M1 could be maintained on stream at a long duration of 15 days. This result shows the enhancement of the role of catalyst hydrophobicity in preventing the decline of the catalyst activity under the influence of additional water in the gas stream.

3.4.4. Effect of pore size

The order of BET surface area and pore size of the catalyst supports (Table 1) are as follows: M2 ≈ M3 > M1 ≫ ZSM-5 (BET surface area) and M1 > M3 ≈ M2 ≫ ZSM-5 (pore size). However, in all cases, the oxidation activity of all catalysts displays the following trends: Pt-2/M1 > Pt/M2 ≈ Pt/M3 > Pt/ZSM-5 at temperatures below 200°C and Pt-2/M1 > Pt/M2 ≈ Pt/M3 ≈ Pt/ZSM-5 at temperatures over 200°C. These orders of the catalyst activities are different from the order of the catalyst surface area but are quite similar to the order of the catalyst pore size. This result shows that the catalyst activity is dependent on the pore size, as there is a smaller resistance for diffusion of reactants/products in and out of the larger pores, leading to higher catalyst activity.

4. Conclusion

The oxidation of aromatics on Pt/MCM-41 catalyst is related to the structure of the organic substrates, with the trend of the oxidation activity as follows: toluene > benzene > cumene > ethyl benzene > mesitylene. Among the Pt/MCM-41 catalysts, the most hydrophobic Pt-2/M1, which was prepared under fluoride medium, gives the highest conversion for toluene and is the least affected by the additional water in the gas stream. The order of the activity of catalysts for toluene oxidation is Pt-2/M1 > Pt/M2 ≈ Pt/M3 > Pt/ZSM-5 at temperatures below 200°C and Pt-2/M1 > Pt/M2 ≈ Pt/M3 ≈ Pt/ZSM-5 at temperatures above 200°C. In the presence of the additional

water vapor in the gas stream, the order of the catalyst activity becomes Pt-2/M1 > Pt/M2 > Pt/M3 > Pt/ZSM-5 (at temperatures below 250°C) and becomes Pt-2/M1 > Pt/M2 ≈ Pt/ZSM-5 > Pt/M3 (at temperatures above 250°C). These results show that the oxidation activity of catalysts is mainly dependent on the surface hydrophobicity of the catalyst support and partially dependent on the pore size of the catalyst.

Based on the above reaction and characterization results, it can be concluded that the hydrophobicity and pore size of catalysts are crucial for the combustion activity of the catalyst. The catalyst hydrophobicity can be enhanced through the synthesis of the catalyst support in fluoride anions.

References

[1] E. Noordally, J.R. Richmond, S.F. Tahir, Catal. Today 17 (1993) 359.
[2] R.M. Heck, R.J. Farrauto, Catalytic Air Pollution Control: Commercial Technology, International Thomson Publishing, New York, 1995, p. 435.
[3] J. Spivey, Ind. Eng. Chem. Res. 26 (1987) 2165.
[4] G.I. Golodets, Heterogeneous Catalytic Reactions Involving Molecular Oxygen, Elsevier, New York, 1983, p. 234.
[5] J. Volter, G. Lietz, H. Spindler, H. Lieske, J. Catal. 104 (1987) 375.
[6] R. Burch, Catal. Today 35 (1997) 27.
[7] Y.F. Yao, I & EC Prod. Res. Dev. 19 (1980) 293.
[8] K.T. Chuang, B. Zhou, S. Tong, Ind. Eng. Chem. Res. 33 (1994) 1680.
[9] K.T. Chuang, S. Cheng, S. Tong, Ind. Eng. Chem. Res. 31 (1992) 2466.
[10] H.A. Rangwala, S.E. Wanke, F.D. Otto, Can. J. Chem. Eng. 72 (1994) 296.
[11] J.C.S. Wu, T.Y. Chang, Catal. Today 44 (1998) 111.
[12] B. Natari, Adv. Catal. 41 (1996) 253.
[13] C. Lahouse, A. Bernier, P. Grange, B. Delmon, P. Papaefthimiou, T. Ioannides, X. Verykios, J. Catal. 178 (1998) 214.
[14] M. Paulis, L.M. Grandia, A. Gil, J. Sambeth, J.A. Odriozola, M. Montes, Appl. Catal. B: Environ. 26 (2000) 37.
[15] P. Papaefthimiou, T. Ioannides, X.E. Verykios, Appl. Catal. B: Environ. 13 (1997) 175.
[16] J.S. Beck, J.C. Vartuli, W.J. Roth, C.T. Kresge, K.D. Schmitt, J. Am. Chem. Soc. 114 (1992) 10834.
[17] I.M. Dahl, E. Myhrovold, A. Slagtern, M. Stocker, Adsorb. Sci. Tech. 15 (1997) 289.
[18] C.J. Brinker, G.W. Scherer, Sol–Gel Science, Academic Press, London, 1990, p. 582.
[19] Q.H. Xia, K. Hidajat, S. Kawi, Mater. Lett. 42 (2000) 102.
[20] R.B. Borade, A. Clearfield, Catal. Lett. 31 (1995) 267.
[21] J.L. Guth, H. Kessler, R. Wey, Stud. Surf. Sci. Catal. 28 (1986) 121.
[22] Y.C. Long, Y.J. Sun, H. Zeng, J. Inclu. Phe. 28 (1997) 1.
[23] A. Corma, V. Fornes, M.T. Navarro, J. Perez-Pariente, J. Catal. 148 (1994) 569.
[24] A. O'Malley, B.K. Hodnett, Catal. Today 54 (1999) 31.
[25] R.K. Sharma, B. Zhou, S. Tong, K.T. Chuang, Ind. Eng. Chem. Res. 34 (1995) 4310.